International Astronautical Congress, Sydney, Australia, 29 September - 3 October 2025.

IAC-25 C4 7 11 x96455

Design and Testing of a Ramjet as a Second Stage for Small Scale Rocket Models

Francesco Margani[a,b]*, **Luca Armani**[a,b], **Riccardo Nicoletti**[a,b], **Ben Shoesmith**[a], **Marin Le Guennec**[c], **Antonella Ingenito**[a]

[a] *Advanced Space Propulsion Laboratory, Sapienza University of Rome, Italy*

[b] *GAUSS srl, Italy*

[c] *Institut Polytechnic de Paris*

* Corresponding author

Abstract

Airbreathing propulsion technologies play a crucial role in both civil and military aerospace applications due to their high efficiency in atmospheric flight. Unlike traditional rocket propulsion, which relies on onboard oxidizers, a ramjet utilizes atmospheric oxygen, potentially improving overall system efficiency and reducing launch weight. The proposed ramjet is optimized for a cruise Mach, with design parameters including inlet ramp angles, pressure losses, and combustion efficiency carefully selected to maximize performance. A detailed analysis is conducted on the air inlet system, combustion chamber geometry, and nozzle configuration to ensure stable operation across the expected flight envelope. Special attention is given to the selection of fuel and ignition strategies to guarantee reliable startup and sustained combustion under varying flow conditions. Following the conceptual and computational design phase, a scaled prototype was fabricated using high-resolution 3D printing. Experimental testing was conducted in a controlled environment to evaluate key performance parameters, with a particular focus on new configuration rocket model stability and overall thrust production. The outcomes of this research will provide valuable insights into the feasibility of integrating ramjet technology into small-scale orbital launch systems, potentially offering a cost-effective and efficient alternative to conventional rocket staging strategies.

Nomenclature

M = Mach number
γ = Specific heat ratio
η_p = Stagnation pressure ramps efficiency
θ = Ramp angle
β = Shock wave angle
p_t = Stagnation pressure
M_n = Normal Mach number to the shock
ρ = Air density
C_d = Drag coefficient
A = Reference area of rocket cross-section
$Y(t)$ = Altitude
$V(t)$ = Velocity
$a(t)$ = Acceleration
$D(t)$ = Aerodynamic drag force
$M(t)$ = Rocket mass
$\dot{m}$ = Propellant mass flow rate
t_{bo} = Burnout time

Acronyms/Abbreviations

PLA-CF = Polylactic Acid with Carbon Fiber
CFD = Computational Fluid Dynamics
MSE = Mean Squared Error
SST = Shear Stress Transport (turbulence model)
CFL = Courant–Friedrichs–Lewy number
CAD = Computer-Aided Design
IMU = Inertial Measurement Unit

1. Introduction

Ramjet engines represent one of the most efficient propulsion systems for achieving sustained supersonic flight, playing a critical role in both civil and military aerospace applications. One of the primary challenges in ramjet design lies in the development of an efficient inlet capable of operating effectively across the entire flight envelope. The inlet must ensure optimal compression of the incoming airflow while minimizing losses and avoiding flow separation, which could compromise the performance

of the combustion chamber.

In this context, oblique shock theory and the Rankine–Hugoniot relations are commonly employed to evaluate the trade-offs between mass flow rate and pressure losses induced by oblique and normal shocks. Proper design ensures that the boundary layer remains attached, preventing adverse effects such as flow detachment and pressure losses, thereby maintaining favorable conditions for combustion in terms of both pressure and temperature.

To experimentally evaluate the inlet performance, the design will be integrated into the ogive-shaped nose cone of the rocket model. A dedicated sensor system will be integrated to measure pressure and temperature at critical locations along the inlet, providing detailed data to assess its aerodynamic efficiency and flow behavior.

This study specifically focuses on assessing the performance of a ramjet inlet optimized for a flight Mach number of 1.8, based on the selected rocket configuration. The primary objective of the analysis is to maximize the mass flow rate delivered to the combustion chamber while minimizing pressure losses associated with shocks and boundary layer effects. Accurate characterization of these parameters is essential for ensuring optimal combustion conditions, thereby improving the overall propulsion efficiency and effectiveness of the ramjet system.

2. Ramjet Inlet Design

2.1 Design of Inlet Ramp Angles

The ramjet will have to operate at speeds between Mach 1.6 and 2.0 at 6 kilometers of altitude. A Mach number of 1.8 is assumed for the inlet fluid velocity in the design. So the operating condition of the ramjet in terms of pressure, density and temeprature are summerizex in Table 1.

M_∞	p_∞ (bar)	ρ_∞ (kg/m^3)	T (K)	γ
1.8	0.47	0.66	249	1.4

Table 1: Input data for the ramjet operating conditions at 6 km altitude.

The inlet of a ramjet engine plays a crucial role in enabling efficient high-supersonic flight by decelerating and compressing the incoming airflow. This process must be accomplished while minimizing total pressure losses and aerodynamic drag. Optimal inlet design typically employs oblique shocks generated by compression ramps, which provide effective flow compression with minimal energy [1] [2].

The efficiency of the ramp-compression process is expressed as

$$\eta_p = \frac{p_{t5}}{p_{t0}} \tag{1}$$

where p_{t5} is the average stagnation pressure at the entrance to the combustor and p_{t0} is the stagnation pressure in the freestream. For supersonic flow over a wedge, the relationship between the flow deflection angle θ, the shock wave angle β, and the upstream Mach number M is described by the θ–β–M relation:

$$\tan\theta = 2\cot\beta\,\frac{M^2\sin^2\beta - 1}{M^2(\gamma + \cos 2\beta) + 2} \tag{2}$$

For a given M, this function exhibits a maximum deflection angle $\theta_{\max}$ corresponding to a specific β.

To determine the optimal ramp configuration, a systematic investigation of different deflection angles was carried out in order to identify the best compromise between compression efficiency and aerodynamic drag reduction. The performance of each configuration was evaluated in terms of total pressure recovery and shock-induced losses, and an iterative procedure was employed following the methodology described in [3] to refine the ramp geometry and maximize inlet performance.

The final design target is an inlet operating at $M = 1.8$ with zero angle of attack, ensuring maximum stagnation pressure recovery. Particular attention is given to the behavior of the shocks generated at the cowl lip, which must remain attached over the entire operating range, both for the internal and external surfaces of the cowl. Additionally, a mechanical constraint is imposed, setting a minimum allowable wedge angle of 5°.

In inlet compression systems employing oblique and normal shock waves, the highest efficiency η_p is achieved when all oblique shocks have the same strength. This condition is satisfied when the Mach number normal to each shock is identical, a principle known as the Oswatitsch criterion [4]:

$$M_n = M\sin(\beta) = \text{const.} \tag{3}$$

where M_n denotes the Mach number normal to the shock. In practice, however, maximum values of η_p are obtained when the Mach number upstream of the terminal normal shock is approximately 94% of the Mach number normal to the preceding oblique shocks.

The selected configuration is based on two oblique shocks followed by a terminal normal shock [4], resulting in a stagnation pressure ratio of $\eta = 0.978$. The corre-

sponding dimensionless ramp parameters are summarized in Fig.(1).

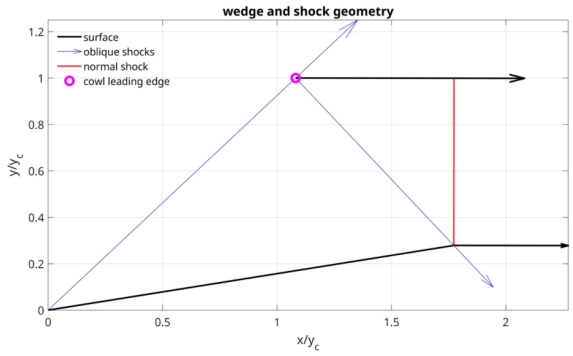

Fig. 1: Theoretical ramp system and shock pattern.

The main drawback of this design is that it features a finite internal contraction ratio that exceeds the Kantrowitz limit [5], which defines the maximum allowable contraction area capable of accommodating the incoming supersonic flow. As a result, the inlet would not be able to start reliably under the designed operating conditions. To overcome this limitation, the throat area is increased so that the effective area ratio satisfies the Kantrowitz criterion, thereby ensuring that the inlet is started at Mach 1.6 (form the beginning of the test).

2.2 CAD model

After sizing the ramps, a dedicated design process was undertaken to optimally integrate the ogive from the baseline rocket configuration with the new geometry, which includes the ramps and the inlet. Particular attention was paid to minimizing the additional mass to preserve the overall weight of the rocket, maintain stability, and ensure that the required Mach number could be achieved at the target altitude.

The inlet, as described in Section 2.1, is arranged in a back-to-back configuration, such that its inherent symmetry minimizes any adverse effects on the rocket's overall performance.

Given the high speeds and accelerations involved, a two-dimensional ramjet ogive was developed to mitigate potential structural issues. The ogive was fabricated using a 3D printer with PLA-CF, having a density of approximately $1.24\ g/cm^3$.

As the ramjet is unpowered and entirely carried by the rocket, air ejection must occur laterally rather than through the base. The nose cone has a total length of 0.5 m; however, the 0.08 m segment at its base is reserved for structural attachment and is therefore unavailable for the ramjet or for air ejection. Within the remaining space, an initial design was developed to enable effective air ejection, nominal ramjet operation, and sufficient air penetration. For this purpose, an inlet dimension of $y_c = 0.02$ m was selected.

The chosen inlet dimension guided the determination of the combustion chamber length and the geometry of the ejection section. A length of 0.4 m was selected, providing sufficient space for the remaining components, particularly the ejection system. This approach aligns with conventional ramjet design principles and ensures consistency with operational models.

A critical aspect of the design concerns the combustion chamber and the exit section. Since the parachute is housed inside the rocket model, the nose cone cannot be separated from the rest of the structure. Consequently, the flow outlet was designed with a curved profile, which represents the most effective solution to minimize aerodynamic drag and prevent undesirable effects on the experimental results. The final CAD model, constrained to fit within the predefined nose cone geometry, is shown in Figs (2) and (3).

To further satisfy the project requirements, an additional modification was introduced. The ramjet is intended to reproduce the aerodynamic behavior of a functional engine, but without combustion. For this reason, an ejection section was added to the design, with the aim of altering the flow as late as possible. In particular, the decision was made to avoid keeping the flow split into two separate streams at the nozzle exit, since this does not reflect the operation of a real ramjet. Instead, the separation into two distinct channels was delayed, allowing the flows to merge before exiting, thus ensuring a more realistic aerodynamic situation.

The design will be refined subsequently to more closely approximate a functional ramjet, particularly by reducing the size of the central section.

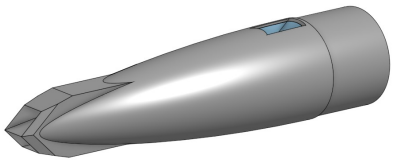

Fig. 2: Ramjet ogive CAD model

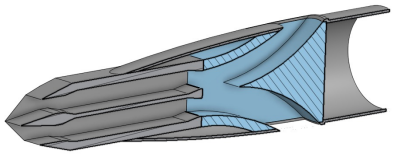

Fig. 3: Section ramjet ogive CAD model

2.3 CFD validation

To validate the design, a computational fluid dynamics (CFD) analysis was conducted. Initially, a two-dimensional CFD study was performed to evaluate the efficiency of the inlet and to verify the correct sizing of the ramps. This preliminary 2D analysis allowed for a detailed assessment of the internal flow characteristics, identifying potential regions of flow separation, shock formation, and pressure losses.

For this simulation, a computational domain consisting of approximately 250,000 elements was employed. The analysis was performed under steady-state conditions, using the k-ω SST turbulence model, which is well-suited for capturing both near-wall effects and adverse pressure gradients. A second-order upwind scheme was selected for spatial discretization, and a Courant–Friedrichs–Lewy (CFL) number of 0.5 was adopted to ensure numerical stability and convergence. The inlet is modeled as a pressure far-field boundary condition, with the corresponding data summarized in Table 1.

The results of the CFD analysis are presented in Fig. (4), illustrating the distribution of Mach number, pressure, and temperature within the ramjet. These results provide a quantitative assessment of the aerodynamic performance of the inlet and ramps, confirming the suitability of the chosen geometry for the intended operational conditions.

After the 2D analysis, it is essential to perform a comparison with a 3D simulation in order to evaluate the influence of all the components of the rocket. In this case, a spherical computational domain was created around the rocket with the ramjet ogive, consisting of approximately 1.5 million elements. The turbulence model was set to k-ω, and an upwind second-order AUSM scheme was employed for the numerical solution.

Fig. (5) shows the Mach number distribution for the 3D ramjet nozzle ogive. This visualization allows the observation of both the external shock structures and the internal flow characteristics, providing a comprehensive

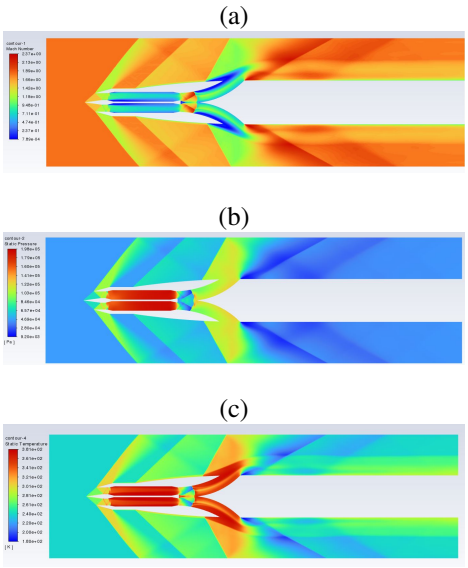

Fig. 4: 2D ramjet ogive CFD contour for Mach number (a), static pressure (b) and static temperarture (c). Inlet conditions are summerized in Tab. 1.

understanding of the flow behavior around the rocket.

It is possible that the first shock does not reach exactly the cowl lip in the 3D simulation. This behavior can be attributed to several factors. First, the mesh refinement is necessarily limited due to the high computational cost, which can affect the resolution of shock structures. Additionally, the presence of the lateral walls may influence the flow at the inlet, slightly altering the shock position compared to idealized or 2D simulations. Despite these limitations, the simulation still provides valuable insights into the overall flow behavior and shock interactions within the ramjet inlet.

3. Rocket design

The original rocket prototype was designed using OpenRocket software. It has been relized in collaboration with ACME Italia. The configuration corresponds to a single-stage launch vehicle equipped with three carbon-fiber fins, ensuring structural rigidity and aerodynamic stability. The total dry mass of the system, including the ramjet ogive, is approximately 6 kg.

The propulsion system selected for this configuration is the M1939 motor, capable of reaching an apogee of approximately 7 km. The vehicle achieves a maximum Mach number of 1.8, with a supersonic flight regime ($M > 1$) sustained for about 8.37 s during the ascent phase.

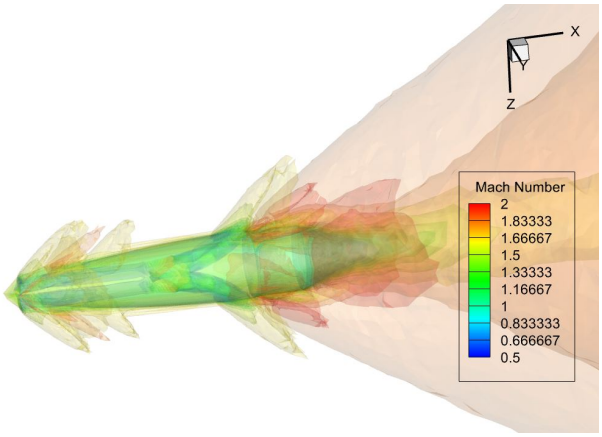

Fig. 5: Mach 3D contour of the ramjet ogive

Fig. 6 illustrates a 1:2 scale model of the rocket, which was employed during preliminary launch tests to evaluate aerodynamic stability and overall flight behavior.

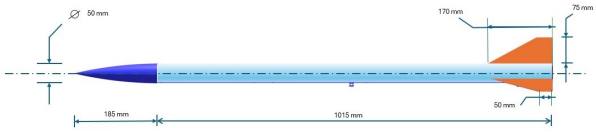

Fig. 6: Original rocket model (1:2 scale).

4. Fight test and stability analysis

Once integrated with the nose cone, the rocket prototype is ready for flight. For the first preliminary tests aimed at assessing the aerodynamic stability of the model, a scaled version at 1:2 of the final configuration was manufactured and assembled. This prototype was designed to reach an apogee of approximately 200 m, providing suitable conditions for validating the stability characteristics under realistic flight dynamics. Fig. (7) illustrates the experimental setup prepared for the launch phase.

This section presents the results of three experimental rocket launches conducted on July 27, 2025, in Loreo, Italy.

To record the flight data, a Jolly Logic altimeter [6] was employed. The device combines a barometric sensor, used to measure pressure and altitude, with a three-axis accelerometer. The campaign included two launches using E24 motors, first with a conical nose cone and then with a ramjet-shaped nose, followed by a third launch employing F36 motors with the ramjet nose. Each rocket was equipped with four motors, one of which integrated a separation charge to ensure proper stage release and parachute deployment.

Fig. 7: Rocket model with integrated ramjet ogive ready to flight

The primary objective of the first two launches was to compare the aerodynamic performance of the ramjet-shaped nose against the conventional conical design, while simultaneously verifying flight stability. The third launch was intended to further confirm stability at higher speeds and altitudes. To ensure a fair comparison, the conical nose being lighter than the ramjet nose was ballasted to match its mass.

Regarding data processing, velocity measurements were smoothed using a fourth-order Butterworth low-pass filter with a cutoff frequency of 0.5 Hz, as the raw data were not directly exploitable. In contrast, pressure and total acceleration data were of sufficient quality to be used without filtering. The accelerations measured along the X and Z axes were not included in this analysis, as they did not provide additional relevant insights. Instead, total acceleration was preferred over the Y-axis acceleration alone, in order to account for any misalignment between the sensor's vertical axis and the true Earth-referenced vertical.

Building on these processed datasets, the temporal evolution of the flight can be interpreted by examining the characteristic phases of the trajectory represented respectively in Figs. (9), (10) and (11) :

- 0–1.5 s (boost phase): the acceleration (magenta curve) exhibits a high initial peak, followed by a progressive decrease due to both the quadratic dependence of aerodynamic drag on velocity ($\propto v^2$) and the reduction in propellant mass. The altitude (blue curve) initially increases in a nearly parabolic trend, becoming less steep as burnout approaches.

- ~1.5 s (burnout): propulsion ceases, and the velocity (cyan curve) reaches its maximum value. From this point onward, only gravity and drag act on the vehicle.
- 1.5–~7 s (coast phase): velocity decreases steadily under the combined effects of g and aerodynamic drag, while altitude continues to increase until apogee, where the slope of the altitude curve vanishes.
- Ejection delay (~7 s): the C6 motor features a nominal delay of about 7 s, so ejection occurs just after apogee (orange curve, Chute). If the ejection is slightly delayed relative to apogee, a short ballistic descent is observed before parachute deployment.
- Parachute descent: altitude decreases almost linearly, corresponding to the system's terminal descent under parachute. Small irregularities or steps can be attributed to wind gusts.
- Velocity/acceleration spikes: the narrow peaks in velocity (cyan) and acceleration (green) are consistent with sensor noise (IMU/barometric) or minor aerodynamic disturbances, rather than actual physical accelerations of the rocket body.

Some key phases of the flight are illustrated in Fig. (8).

(a) Launch phase (b) Mid-flight (c) Parachute open

Fig. 8: Relevant flight phases.

To evaluate the aerodynamic performance of the newly designed ogive, a comparative analysis is carried out against the reference configuration. The comparison is performed in terms of key dynamic parameters, namely acceleration, velocity, and drag coefficient C_d. This approach allows for a comprehensive assessment of the influence of the ogive geometry on the overall flight performance, highlighting both potential improvements and possible trade-offs between the two configurations.

Both using the E24 and the F36 motor, the stability of the rocket model has been thoroughly evaluated and confirmed, with no critical issues observed when employing the ramjet ogive. Figs. (12a) and (12b) present a comparison of the

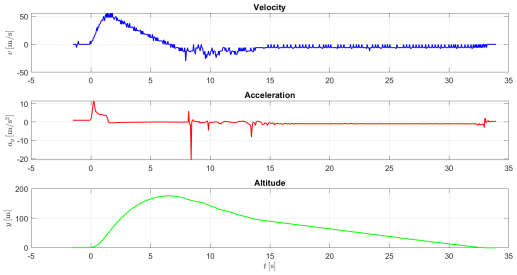

Fig. 9: Test 1 with normal ogive and E24 motor

Table 2: Characteristics of the rocket, engine, and flight performance (standard configuration).

Parameter	Value	Unit
Rocket		
Lift-off mass	0.386	kg
Drag coefficient, C_d	0.60	–
Diameter	0.050	m
Engine		
Average thrust	23.0	N
Burn time	1.47	s
Delay time	7.00	s
Total engine mass	0.084	kg
Propellant mass	0.042	kg
Total impulse	33.81	N·s
Performance		
Maximum altitude	176	m
Maximum velocity	57.8	m/s

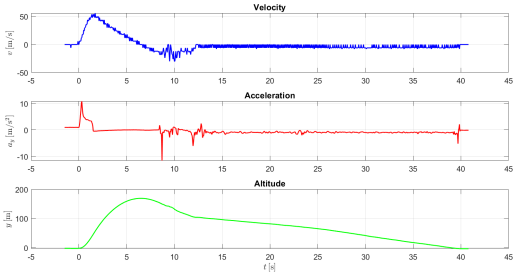

Fig. 10: Test 2 with ramjet ogive and E24 motor

altitude and velocity, respectively, achieved in the three different tests.

The estimation of the ogive drag coefficient is particularly critical, since the measurement noise affecting the sampled data is not negligible. For this reason, the raw measured data alone are not sufficiently reliable for an ac-

Table 3: Characteristics of the rocket, engine, and flight performance (Ramjet ogive configuration).

Parameter	Value	Unit
Rocket		
Lift-off mass	0.386	kg
Drag coefficient, C_d	0.68	–
Diameter	0.050	m
Engine		
Average thrust	23.0	N
Burn time	1.50	s
Delay time	7.00	s
Total engine mass	0.084	kg
Propellant mass	0.042	kg
Total impulse	34.5	N·s
Performance		
Maximum altitude	171	m
Maximum velocity	57.2	m/s

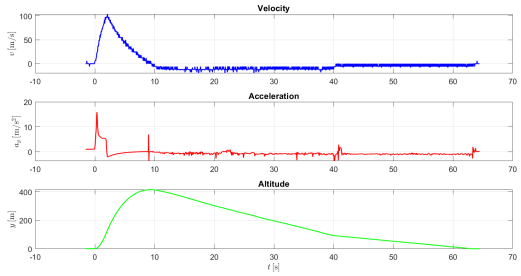

Fig. 11: Test 3 with ramjet ogive and F36 motor

curate determination of C_d.

To address this issue, the adopted methodology relies on recalculating the acceleration and velocity profiles through the rocket dynamic equation [7] [8]. From these results, the drag coefficient is then identified by estimating the trajectory and selecting the value of C_d that minimizes the Mean Squared Error (MSE). For an accurate determination of C_d, it is essential to consider the initial powered phase of the flight, where thrust is present, in order to evaluate acceleration and velocity. These data are subsequently employed to validate the coefficient during the inertial ascent phase.

Table 4: Characteristics of the rocket, engine, and flight performance.

Parameter	Value	Unit
Rocket		
Lift-off mass	0.386	kg
Drag coefficient, C_d	0.68	–
Diameter	0.050	m
Engine		
Average thrust	32.0	N
Burn time	2.05	s
Delay time	7.00	s
Total engine mass	0.108	kg
Propellant mass	0.064	kg
Total impulse	65.6	N·s
Performance		
Maximum altitude	412	m
Maximum velocity	105.3	m/s

(a)

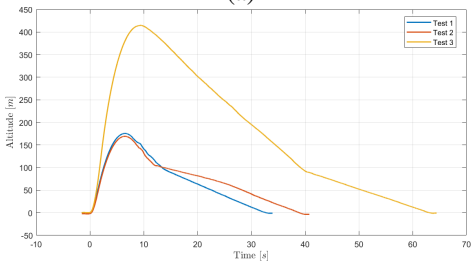

(b)

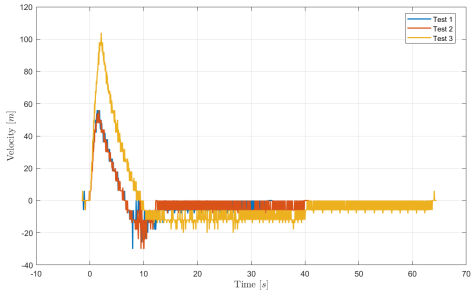

Fig. 12: Altitude and velocity comparison

The governing equations of the rocket dynamics can be expressed as follows:

$$M(t) = \begin{cases} m_0 - \dot{m}\, t, & t \le t_{bo} \\ m_0 - m_{\text{prop}}, & t > t_{bo} \end{cases} \tag{4}$$

$$\rho(t) = \rho\big(Y(t)\big) \tag{5}$$

$$T(t) = \begin{cases} T, & t \le t_{bo} \\ 0, & t > t_{bo} \end{cases} \tag{6}$$

$$D(t) = \tfrac{1}{2}\,\rho(t)\,V(t)^2\,C_d\,A \tag{7}$$

$$a(t) = \frac{T}{M(t)} - g - \frac{D(t)}{M(t)} \tag{8}$$

$$V(t+\Delta t) = V(t) + a(t)\,\Delta t \tag{9}$$

$$Y(t+\Delta t) = Y(t) + V(t)\,\Delta t \tag{10}$$

where $M(t)$ is the vehicle mass, $\rho(t)$ is the atmospheric density at altitude $Y(t)$, $T(t)$ is the engine thrust, $D(t)$ is the aerodynamic drag force, $a(t)$ is the vehicle acceleration, $V(t)$ is the velocity, and $Y(t)$ is the altitude.

Since the drag coefficient C_d is not known a priori, a parametric approach is adopted. Several trajectories are numerically simulated by varying C_d within the range 0.1 to 1.5, with increments of 0.01. For each simulated trajectory, MSE between the computed trajectory and the experimental measurements is evaluated. The optimal drag coefficient is then identified as the value of C_d that minimizes the MSE. This procedure is systematically applied to all three configurations under investigation, ensuring a consistent and objective estimation of C_d. The comparison for the measured and analytical altitude for one case is represented in Fig. 13

The drag coefficient for the standard ogive is $C_d = 0.6$, whereas for the ramjet ogive it increases to $C_d = 0.68$, corresponding to an approximate 13% increase. This increment, although noticeable, is considered acceptable for this type of application, as it does not compromise the overall flight performance or stability margins. Moreover, the slight increase in drag is expected given the geometrical modifications required for the ramjet integration, and it remains within the typical range for comparable configurations. These results suggest that the ramjet ogive can be used without significant penalties in aerodynamic efficiency, while providing the additional functional benefits associated with ramjet operation.

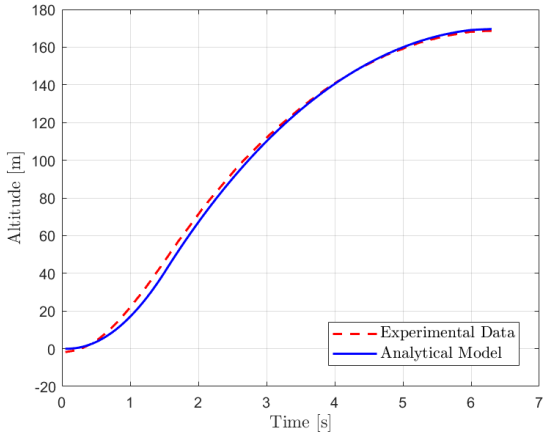

Fig. 13: Analytical and Mesured altitude comparison For Ramjet ogive with C7 motor

5. Conclusions

This work has presented the design, numerical validation, and preliminary experimental testing of a ramjet inlet model that was integrated into the nose of a small scale rocket model. This approach is conceived as a first step toward the integration of airbreathing propulsion into experimental demonstrators. The inlet design was optimized using shock-expansion theory and validated through both two-dimensional and three-dimensional CFD analyses, confirming the ability of the configuration to provide adequate compression and stable flow conditions for subsequent combustion. A CAD model was then realized and manufactured via additive techniques, ensuring compatibility with the baseline rocket configuration and preserving mass and aerodynamic balance.

The integration of the ramjet ogive into scaled rocket models enabled the execution of preliminary flight tests, which demonstrated the overall aerodynamic stability of the system and highlighted only a moderate increase in drag compared to a conventional conical nose cone. The experimental campaign confirmed that the ramjet configuration can be adopted without compromising flight dynamics, thereby validating the design approach and its applicability to future scaled demonstrators. These results represent a significant milestone, as they provide both numerical and experimental evidence of the feasibility of employing ramjet-based solutions in small-scale rocketry.

Building upon these achievements, the next step of the research will consist in the realization of a full-scale (1:1) rocket demonstrator, designed to reach altitudes of up to 6 km. This configuration will integrate a dedicated sen-

sor suite for the measurement of pressure, temperature, and flow parameters at critical locations along the inlet and within the combustion chamber, with the objective of experimentally validating the theoretical and numerical predictions. The acquisition of high-fidelity flight data will provide a deeper understanding of the aerodynamic behavior of the inlet and its ability to sustain favorable combustion conditions.

In a subsequent phase, ignition and combustion tests will be performed in order to assess the capability of the system to achieve reliable starting and stable flame holding during supersonic flight. This will represent a crucial step toward the transition from a purely aerodynamic demonstrator to a fully functional ramjet prototype. The progressive development from scaled flight experiments, to full-scale rocket launches with advanced instrumentation, and finally to ignition trials, will establish a robust methodological framework for the integration of ramjet technology into small-scale launch systems.

Overall, this research lays the groundwork for bridging the gap between analytical design and operational implementation of ramjet propulsion. The outcomes not only confirm the aerodynamic feasibility of the proposed configuration but also define a clear experimental roadmap, ultimately supporting the development of cost-effective, efficient, and reliable airbreathing propulsion solutions for future aerospace applications.

References

[1] T. Cain. Ramjet intakes. *NATO Research and Technology Organization*, 2010.

[2] J. Mahoney. *Inlets for Supersonic Missiles*. AIAA Education Series. American Institute of Aeronautics and Astronautics, Washington, D.C., 1991.

[3] L.Armani, R. Nicoletti, F.Margani, A. Ingenito, and B. Shoesmith. Design and optimization of a small scale solid fuel ramjet. *EUCASS conference paper*, 2025.

[4] J. Seddon and E. L. Goldsmith. *Intake Aerodynamics*. Blackwell Science, Oxford, 2 edition, 1999.

[5] A. Kantrowitz and C. Donaldson. Preliminary investigation of supersonic diffusers. *Technical Report NACA-ARC-L5D20, National Advisory Committee for Aeronautics*, 1945.

[6] Jolly Logic. Altimeterthree. https://jollylogic.com/products/altimeterthree/. Accessed: 2025-09-10.

[7] L. N. P. Peri, L. Armani, F. Margani, H. Ogawa, and A. Ingenito. A small launcher including a dual mode ramjet as second stage. In *Proceedings of the IAF Space Propulsion Symposium*, 2024. Presented at the 75th International Astronautical Congress (IAC 2024).

[8] G. P. Sutton and O. Biblarz. *Rocket Propulsion Elements*. Wiley, Hoboken, NJ, USA, 9th edition, 2016.